Proceedings of the Second International Conference on Press-in Engineering 2021, Kochi, Japan – Matsumoto et al (eds)

Dynamic behavior of cantilever tubular steel pile retaining wall socketed in soft rock

S.M. Shafi & J. Takemura
Tokyo Institute of Technology, Tokyo, Japan

V. Kunasegaram
South Eastern University of Sri Lanka, Oluvil, Sri Lanka

Y. Ishihama & K. Toda
Nippon steel corporation, Chiba, Japan

Y. Ishihara
GIKEN LTD., Kochi, Japan

ABSTRACT: Stability against extreme loads, such as earthquakes, water rise behind the wall and its combination, is a major problem in the application of the cantilever steel tubular pipe wall (CSTP). Centrifuge model tests were carried out to study the mechanical behavior of the CSTP wall with a retain height H=12m and a pipe diameter Φ=2m subjected to such extreme loads in 50g for two different wall socket depth (d_c) of 3 m and 2.5 m. Sequential loadings were applied to the wall with cohesionless backfill (dry & wet). Apart from these loadings, white noises were applied before each load to confirm the dynamic characteristics of the wall. The stability of the wall against dynamic and static loads has been significantly increased by 0.5 m increase in socket depth, and the resilience of the wall has been ensured until the end of the sequential loads for the wall with d_c=3.0m.

1 INTRODUCTION

The cantilever retaining wall is one of the old geotechnical structures used to retain earth with moderate height. These structures are interesting as their stability relies on the generation of the earth pressures on either side of the wall which is based on the complex soil-structure interaction. An extensive research has been done to investigate this complex soil-structure interaction (Terzaghi 1934a, b; Bica and Clayton 1998; Madabhushi et al 2005). However, those studies work on the static loading condition. So, by following the Rankine or Coulomb earth pressure, adequate design safety can be provided to the wall.

The soil structure becomes more complex when the wall is under dynamic loading. The wall may behave mysteriously when subjected to dynamic loading. The general design practice which is based on stress, for example, the famous pseudo-static approach by Mononobe-Okabe (1929) is adopted by the designer in the early stage. A recent research revealed that the stress-based approach may give an over-conservative design. Steedman (1998) suggested that the stress-based design approach will underestimate the lateral displacement. So, it is important to understand not only the earth pressure generated behind the wall but also the wall displacement mechanism for the stability of the retaining wall under dynamic loading. Also, the characteristics of the retaining wall (rigid or flexible) govern the wall behavior. Terzaghi (1934 a) explain a generation of pivot point near the base of the relatively stiff sheet pile wall. The passive earth pressure generated below the retaining wall changes its regime below the pivot point. According to the 1g experiment conducted by Bica and Clayton (1998) on cantilever retaining wall, showed that the earth pressure below the pivot point was smaller than the Rankine passive earth pressure as the wall friction acted downward below the pivot point. So, it is essential to provide a sufficient penetration depth to the retaining wall so that the passive earth pressure generated below the retaining wall can provide stability to the wall.

Current design practice in Japan is based on the famous Chang's (1937) equation which limits the minimum embedment depth required by (2.5β~3β) where β is the characteristics value obtained by the equation:

DOI: 10.1201/9781003215226-30

$$\beta = \sqrt[4]{\frac{k_H B}{4EI}} \qquad (1)$$

where,

k_H= Horizontal subgrade modulus
B= Width of sheet pile
E= Young's modulus of steel.

One of the major limitations of this method is that the required embedment depth is based on the flexural rigidity (EI) of the wall without considering the wall height, and the design is based on the elastic linear behavior. It does not consider the nonlinear soil structure relationship observed in the real field. Also, when the wall height increases the lateral earth pressure increases which will yield large deflection. One way to prevent this large deflection is by increasing the flexural rigidity of the wall, for example, circular pipe wall with a large diameter, but the embedment depth will increase as well. This large embedment depth may not be economical considering the construction point of view. Also, if the structure becomes more rigid, then its application becomes limited to a comparatively stiff ground condition like a soft rock which will make the construction process much harder. Through cutting-edge technology like Gyro-press, it is made possible to install circular pipe wall into the stiff ground yet the cost of construction may not be economical every time if the embedment depth and the length of the wall are comparatively large.

Cantilever retaining wall is normally used to retain moderate height Madabhushi et al (2005); B. V. S. Viswanadham (2009) Different researcher has conducted a study on the cantilever retaining wall with a large retain height with cohesionless backfill soil and penetrating dense sand Jo et al. (2014;2017). Also, Madabhushi et al (2006) conduct a comprehensive numerical analysis for dry and saturated cohesionless backfill as saturated backfill soil may cause structural failure due to high stress or may cause large deformation which will lose the serviceability of the wall. This research includes a large diameter cantilever type steel tubular pipe (CSTP) wall with a wall height H =12m and a pipe diameter Φ=2m embedded in artificially prepared soft rock with embedment depths of 1.25Φ & 1.5Φ. The behavior of the retaining wall has been investigated under static and dynamic loading with dry and wet backfills conditions.

The main intention of this model study is to investigate the dynamic stability of a steel tubular pile wall embedded in soft rock with relatively small embedment depth than Chang's proposed minimum depth and observe the deformation and failure behaviors. Two different cohesionless backfill conditions like dry backfill and wet backfill condition were maintained. The undrained condition was maintained in the backfill to utilize the maximum of the pore pressure generated behind the wall so that

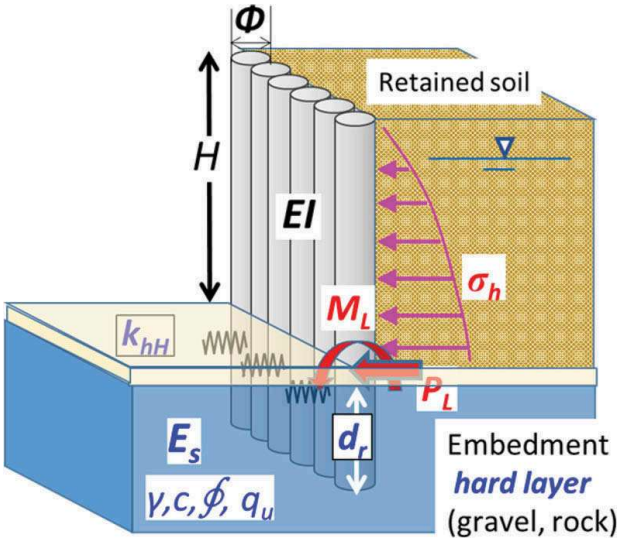

Figure 1. Cantilever retaining wall.

the applied lateral loads on the wall can be increased up to 2.5 times that of the dry backfill condition using the water feeding technique. Figure 1 shows the typical load acting on the wall. Therefore, the stability of the retaining wall was investigated under two extreme loading conditions: large lateral thrust by water feeding and earthquake motion as shown in Figure 1.

2 METHODOLOGY

The description of the model is shown in Figure 2. The whole model was designed for 50g centrifugal acceleration. Different sensors like Leaser Displacement Transducer (LDT), Earth Pressure Cell (EPC), Pore Pressure Transducer (PPT), and Accelerometer, and Strain Gauges (SG) were used to record various responses during the experiment. The wall displacement and force in the forward direction are

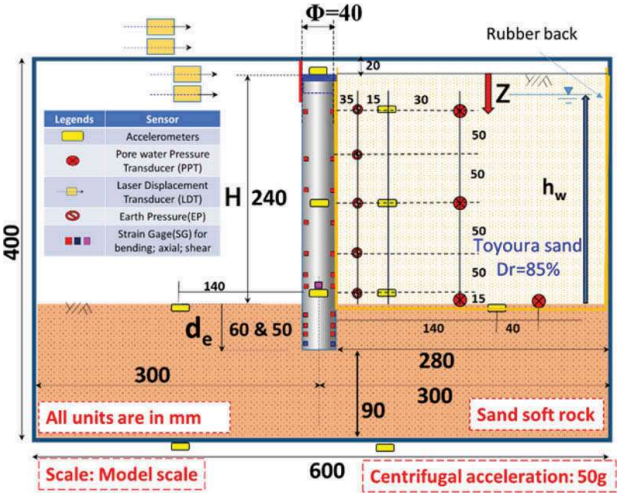

Figure 2. Model setup.

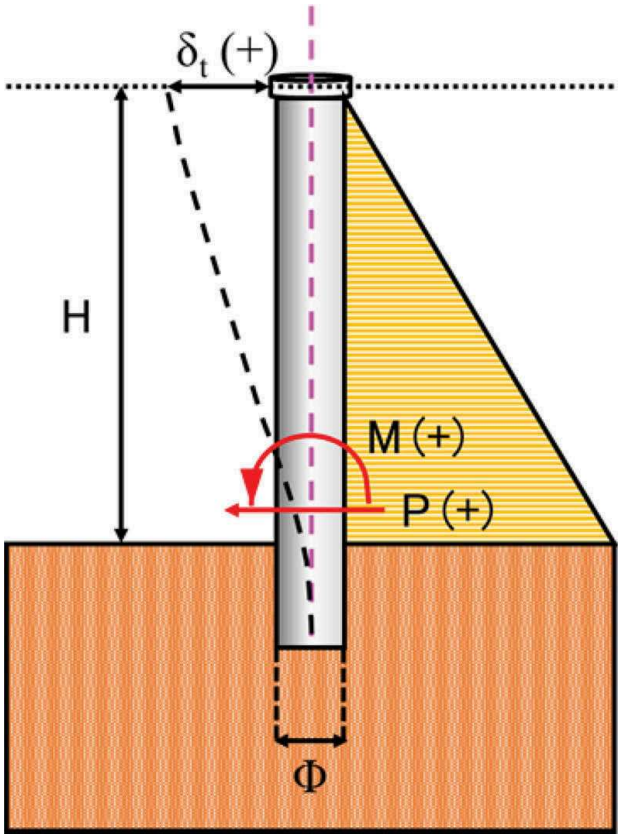

Figure 3. Sign convention used for study.

considered as positive and the anti-clockwise moment is also considered as positive. Different sign assumed for the analysis is shown in Figure 3.

The model container had the original internal dimensions of 600 mm in length, 250 mm in breadth and 400 mm in depth. The container was made up of a removable rear-side aluminum wall and a front-side transparent thick acrylic wall and an aluminum hollow frame to stiffen the acrylic. Both wall plates were bolted with the main container body to form a rigid box. To secure the plane strain conditions and to model the maximum possible width of the wall (max of 5 piles) the breadth of the container was shorten using a lateral acrylic spacer on the inner face of the back-face panel. Before the casting, 0.5 mm thick Teflon sheets were pasted in the front and rear internal container wall faces and lubricated by silicone grease for easy detachment of wall from the hardened soft rock ground.

The artificial soft rock was prepared by mixing cement, sand, clay, and water with a target 14th day unconfined compressive strength of q_u=1.4 MPa. Toyoura sand and Sumi clay were mixed with Portland cement and water to prepare the mixture. The mechanical properties of the artificially prepared soft rock were reported by Vijay et al. (2019) and the main mechanical properties are shown in Table 1 along with the other properties. The soft rock ground was then constructed by compacting the mixture layer by layer at every 30 mm thickness, up to the final height of the planned rock layer with the help of a mechanical vibrator. The density of the compacted mixture was carefully controlled by the volume of each compacted layer and the required mass of the mixture for the layer.

During the preparation of the rock ground, 10 samples were prepared for the unconfined compression test on the 3rd, 7th & 14th days. A mold with a diameter of 50 mm and a height of 100mm was used to prepare the sample. After installation of a pile, in the ground, the ground was covered with a wet towel to avoid any moisture loss. Special care was taken to avoid any crack on the rock surface. After one week, both the container and walls were removed and a new Teflon sheet was attached to the rare wall. 10x10 mm mesh was then made on the front of the ground surface to help in the image analysis. Two days before the test, the gap between the wall was closed by silicon paste so that the surface of the wall facing the backfill may become a uniform plane. After that grease was applied on both sides of the wall in the backfill direction. A membrane rubber bag was used to create an undrained backfill condition as shown in Figure 4 (a). The use of Latex rubber (see

Table 1. Test conditions, and the material properties of wall model.

Test code	Properties of soft rock and sand	Wall height: H_w	Rock socket depth: d_R []: βd_R	Pile Properties Φ, t, EI, M_y
Case 1 (C1)	Toyoura sand (Dr=85%): γ_d=15.8kN/m^3	12m (240mm)	3.0m (60 mm) $^{\$}$ [1.2]	Φ=2 m (40 mm), t = 25 mm (0.5mm) Spacing: 2.15m (43mm)
Case 3 (C3)	ϕ'=42° Soft rock: γ_t=20.1kN/m^3 q_u=1.4MPa E_S=660MPa		2.5m (50mm) [1.0]	EI= 6.8 GNm^2/m (5.4x10^{-5}GNm^2/m) M_y= 9.0 MNm/m (3.6x10^{-3} MNm/m)

βd_R: normalized depth, EI: Pile flexural rigidity, M_y: Bend moment causing pile yielding, ϕ': friction angle from triaxial compression test with σ_3'=98kPa (Tatsuoka et al, 1986) [3)], E_S: Secant modulus of SR (Kunasegaram et al, 2019) [2)] $^{\$}$: Model scales are given in parenthesis

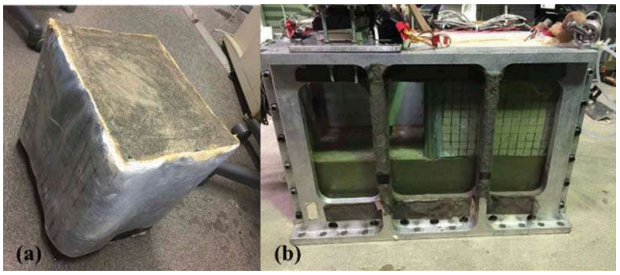

Figure 4. (a) Membrane rubber bag (b) Model before experiment.

Figure 4) bag may create interference of the transmission of the shear stress in between the rock surface and the bottom of the rubber bag. Therefore, to effectively transmit the input accelerations, the rubber membrane bag was designed by using a carbon fiber base (PZ-564 real carbon) at the interface between soil and rock which is also a watertight membrane but quite stiffer compare to the latex rubber.

The prepared rubber bag was then placed behind the wall and filled up with Toyoura sand up to the wall top by maintaining a relative density Dr =85%. The air pluviation method was adopted to fill out the backfill soil so that a uniform dense sand layer can be obtained. While backfilling, different sensors were placed in the backfill soil to measure the earth pressure, acceleration, pore water pressure. The front view of the model before the experiment is shown in Figure 4 (b). Two centrifuge tests were conducted using the Tokyo Tech Mark III centrifuge at a centrifugal acceleration of 50g. Figure 5 shows the detail of the loading sequence along with the typical shape of the input motion. A controlled sinusoidal wave of predominant frequency 1Hz was applied as the input motion for dynamic loading. For this paper, the amplitude of the input motion is defined by the absolute maximum value in the entire time history of the accelerogram and denoted by (a_i). Also, the acceleration in the negative direction is considered as the cause of the forward displacement. The number of the cycle (n_c) referred to the number of effective cycles counted in each shaking. The increment of wall top displacement ($\Delta\delta_t$) for each shaking is also shown in Figure 5. Each case is consisting of three dynamic events along with two static events by water feeding. Case 1 consists of 11 shakings and case 3 consists of 4 shakings. White noise was applied to study the model condition after the application of different loading. The magnitude of the shaking was maintained in such a way that the effect of the loading history could be studied.

3 RESULT AND DISCUSSION

All the results are shown in the prototype scale unless stated otherwise by the author.

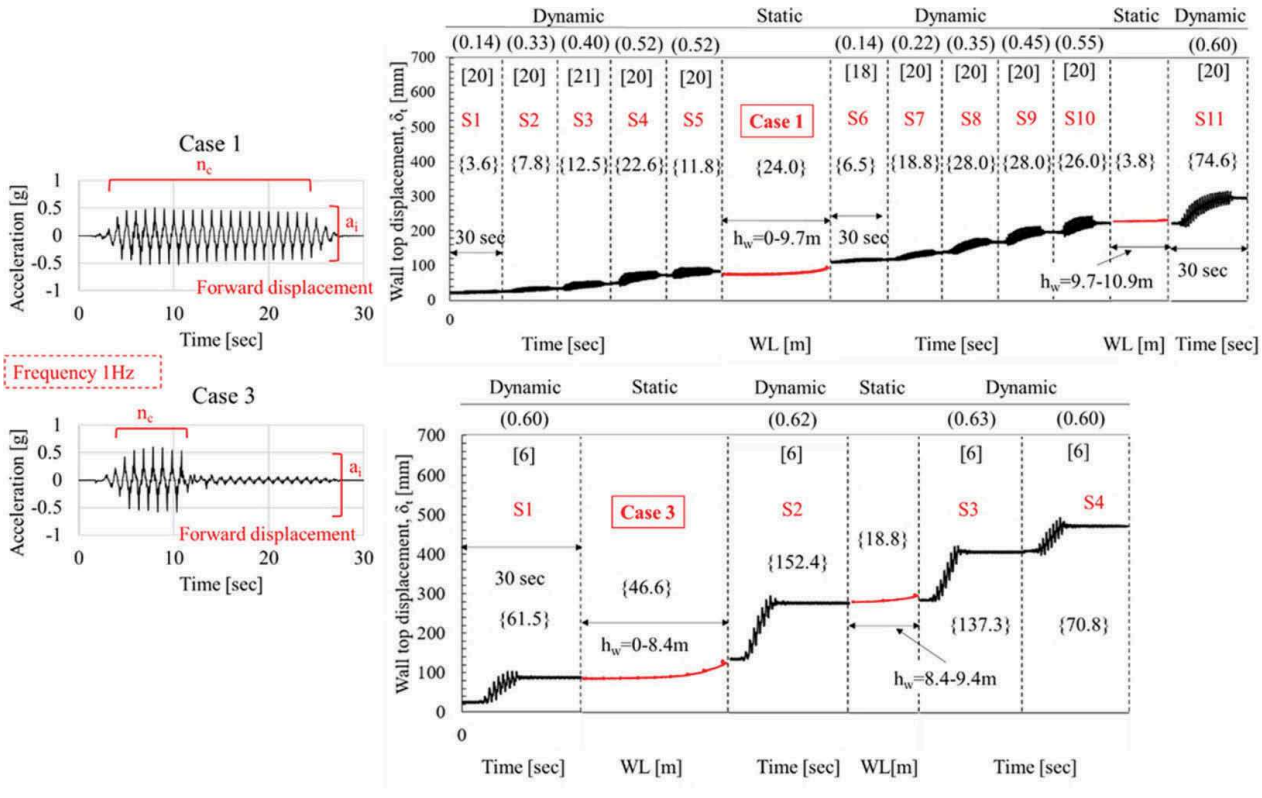

(a_i)= maximum amplitude of input motion (g); [n_c] = no of cycle during the shaking; S1,2,3… = Shake number; { }= $\Delta\delta_t$

Figure 5. Typical shape of input motion, detail of loading sequence and observed wall top displacement.

3.1 *Acceleration response*

Ten accelerometers were installed at various locations of the wall, backfill, rock surface, and container base to record the acceleration response during the dynamic loading as shown in Figure 2. Figure 6 (a), (b) & (c) shows the time history of wall top acceleration, backfill top acceleration and wall top displacement. From Figure 6 (c) it is seen that the maximum accumulation of wall displacement is taking place within the time frame of 5-10 sec. From Figure 6 (d) it is seen that, the wall displacement in forward direction is the combined effect of wall inertia force (acceleration multiplied by negative mass) and lateral earth pressure. Small time lag between the wall acceleration and the backfill acceleration can also be confirmed from the acceleration time history. The peak of the wall acceleration comes earlier than the peak of the earth pressure meaning the wall will push the soil.

The acceleration of all shakings of case 1 & 3 when the inertia force become maximum in forward direction is plotted against the input acceleration (a_i) as defined in Figure 5 is plotted in Figure 6 (e) & (f). It is observed that the acceleration observed in the top of the wall and backfill are over the reference line with slope 1:1 meaning amplification takes place in both wall top and backfill top. Also, it is observed that the amplification in the dry condition is smaller than in the wet condition. One of the reasons could be the addition of water in the backfill soil reduce the predominant frequency of the soil which may cause this large amplification. The amplification in the wall top and the backfill top indicates that the wall and backfill soil do not behave as a rigid body as assumed by the Mononobe-Okabe method. The acceleration response in a dry condition increases almost linearly with the input acceleration meaning the amplification ratio remains almost the same in dry conditions. However, the acceleration ratio in wet conditions tends to decrease for high magnitude input motion.

3.2 *Dynamic displacement behavior of the wall*

To investigate the dynamic behavior of the wall, the displacement, earth pressure, and bending moment time history have been shown in Figure 7. By following the elastic beam theory, bending moment was computed from the bending strain measured from the strain gauge measurement. To show the trends of accumulation of the residual displacement, earth pressure, and bending moment, the moving average of the data recorded during dynamic shaking has been taken and indicated by the thick lines. It is observed that, all the trend lines increase before and

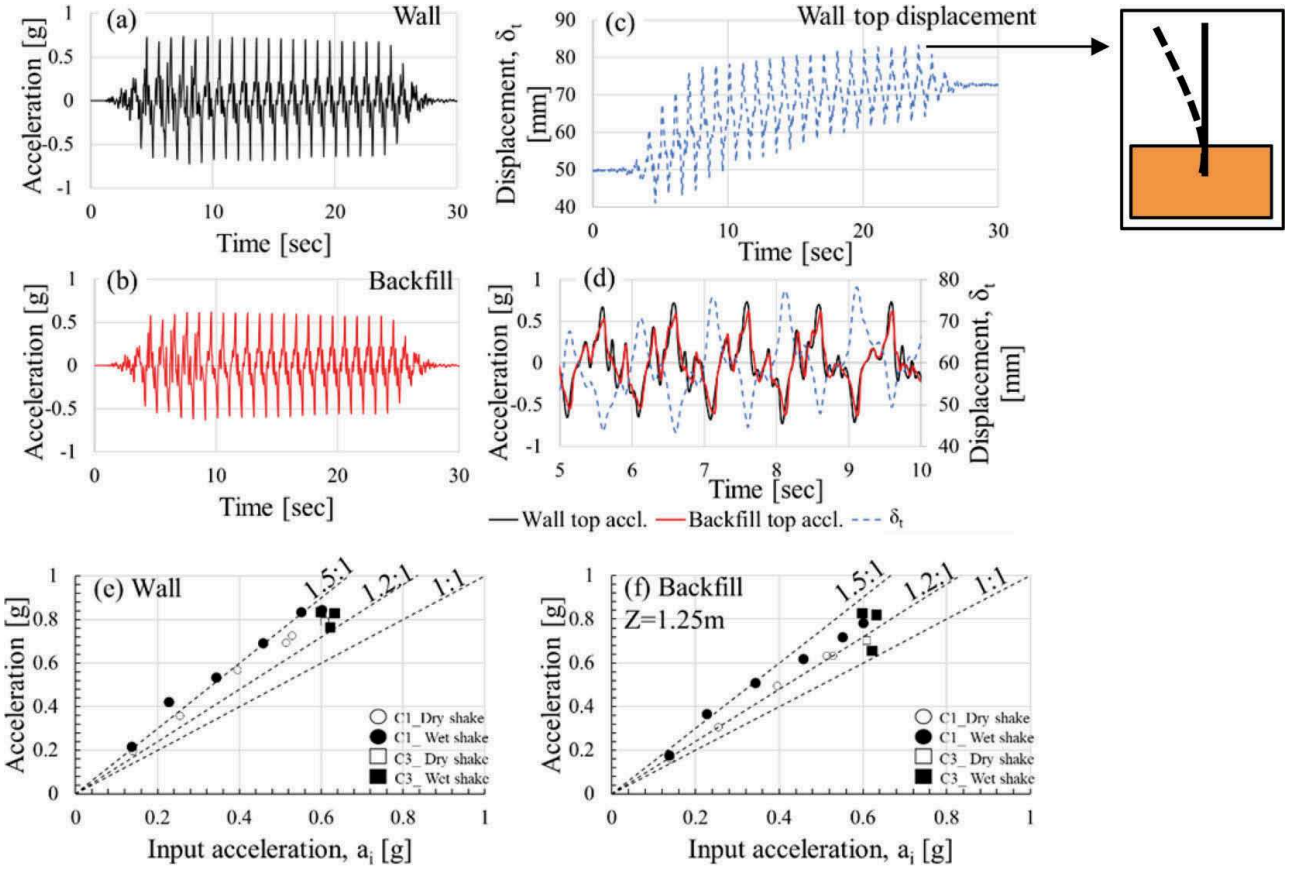

Figure 6. (a)(b)(c) Time history of wall top acceleration, backfill top acceleration and wall top displacement [C1_S4] (d) Relationship between wall and backfill acceleration with wall top displacement [C1_S4] (e)(f) Amplification of wall and backfill top.

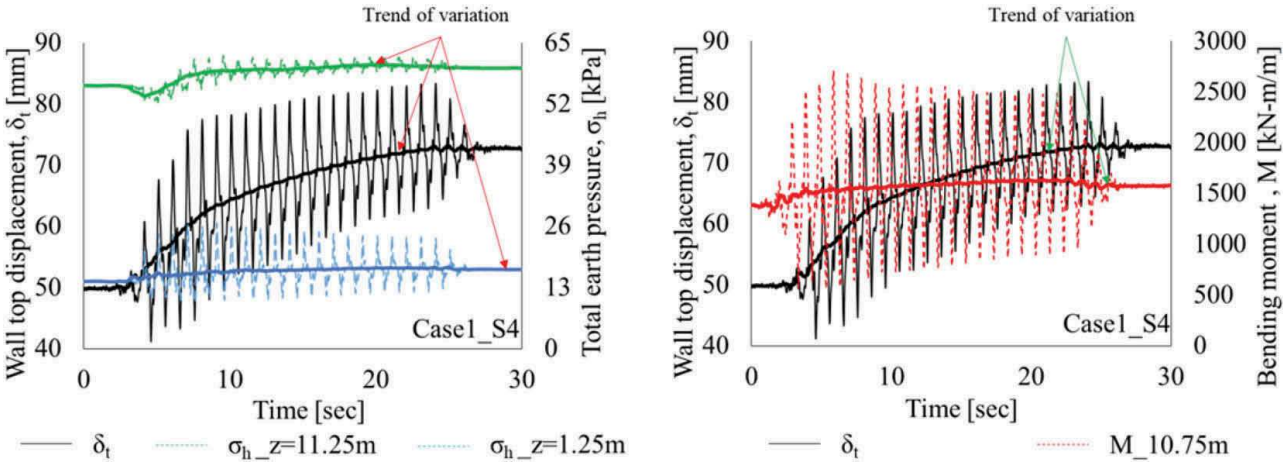

Figure 7. (a) Time history of wall displacement and earth pressure (b) Time history of wall displacement and measured bending moment at 1.25m from rock surface.

after the shaking meaning that accumulation takes place before and after the shaking in displacement, earth pressure, and bending moment measurement.

From the time history of the earth pressure at a shallow and deepest depth, the accumulation of the residual earth pressure is found to be greatest at a deeper depth than at a shallow depth, but the amplification is higher at a shallow depth which makes the shallow depth more critical for the dynamic loading. Small time lag can be seen between the wall displacement and the bending moment response indicating the phase difference occurring between the applied load and the resisting load from the rock surface. In the wall displacement and the earth pressure response, it is seen that the earth pressure increases though the wall displacement is increasing. The mechanism behind this behavior is that due to the wall resilience (property of the wall to move back to its original position) the wall will try to push the soil behind which will create a passive condition thus increase the earth pressure. As the wall requires a large load to push the soil back to its original position that causes a permanent displacement to the wall.

To further investigate the wall displacement behavior, the residual wall displacement increment ($\Delta\delta_t$) has been plotted against arias intensity (A_i) which is defined by equation 2 as shown in the Figure 8.

$$A_i = \frac{\pi}{2g}\int_0^{Td} a(t)^2 dt \qquad (2)$$

where, g is the acceleration due to gravity and Td is the duration of signal above threshold.

For each case, one shake in dry condition and one shake in wet condition are presented in Figure 8. It is seen that the wall displacement during wet shaking is much larger than the dry shaking. The reason behind this behavior is that due to the deterioration of the rock confinement at the later shaking events which yield large displacement. Also, the wall displacement experienced by case 3 is much higher than case 1 which indicates that by changing 0.5m rock socketing depth, accumulation behavior of the residual displacement changes significantly. Observing the trends line for shake 4 & 11 of case one in Figure 8 it can be confirmed that the accumulation of residual displacement which takes place in the earlier part is higher than the later part. A steady increase at the earlier part may expand as the rock confinement deteriorate which is observed in the later shaking (shake 11). To see the effect of the rock socketing depth, the accumulated wall displacement of case 1 and case 3 is plotted against cumulative arias intensity which is defined by Equation 2.

In Figure 9, arias intensity is considered as different shaking was applied to the two models. It is seen that the wall displacement largely increases for case 3 than case 1 though the cumulative arias intensity is much less compared to case 1. Comparing the shake 4 and shake 5 of case 1 and shake 3 and shake 4 of case 3 it is seen that the wall displacement reduced for the later shaking if they are under a similar condition which

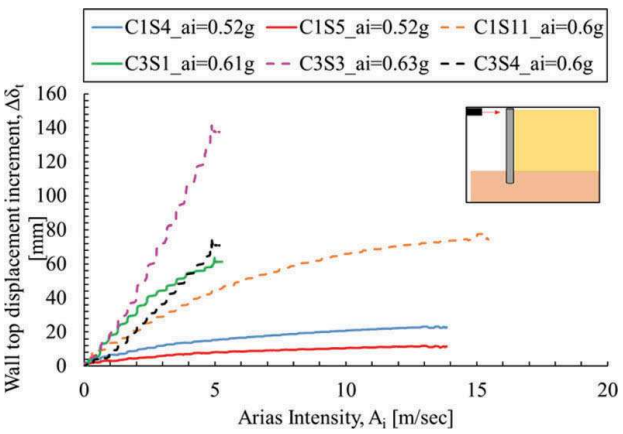

Figure 8. Wall displacement relationship with arias intensity.

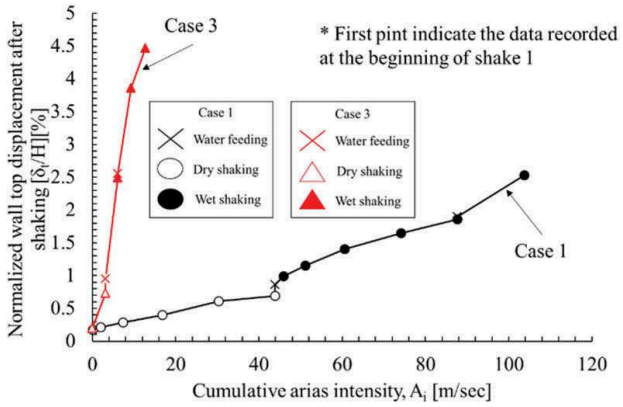

Figure 9. Comparison of wall displacement accumulation behavior of case 1 & 3.

confirms the effect of the wall resilience in the determination of the accumulation of the displacement.

3.3 *Effect of rock socketing depth on the wall behavior*

Comparing Figure 10 (a) & (b), it is seen that the difference in earth pressure before and residual for case 1 is much smaller than case 3. As Figure 10 (a) represents the fourth shaking of case one, due to the previous loading history, the earth pressure doesn't change much which is observed in Figure 10 (b) for the first shake of case 3, where the earth pressure changes from active to at-rest earth pressure. In all the cases, the measured earth pressure at the time of maximum displacement is smaller than the maximum earth pressure recorded by each sensor. However, for the dry backfill condition, the earth pressure distribution is not linear as assumed by the Mononobe-Okabe method.

Figure 11 (a) shows the earth pressure distribution of case 1 for shake 11, and Figure 11 (b) shows the earth pressure distribution for shake 4 of case 3. It is seen that the residual earth pressure experience by case 1 is higher than case 3 which means that the wall of case 1 provides more resistance than case3 which indicates the clear effect of 0.5m rock socketing depth. Also, the earth pressure distribution

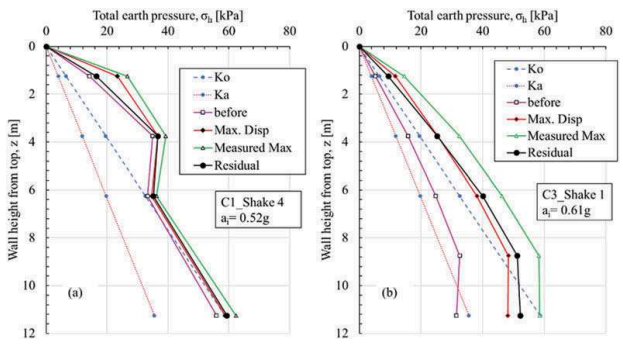

Figure 10. Distribution of earth pressure during dynamic shaking (dry backfill).

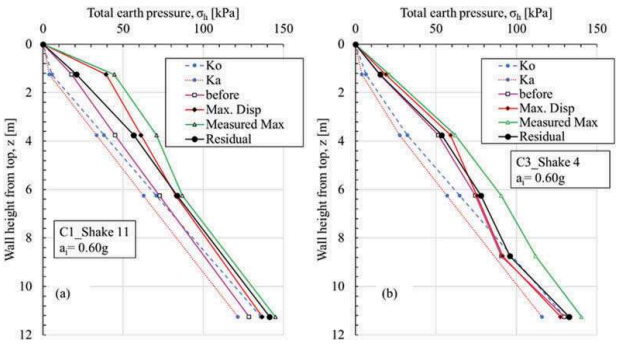

Figure 11. Distribution of earth pressure during dynamic shaking (wet backfill).

significantly increases (more than at-rest earth pressure) in wet shaking compared to dry shaking which justifies the use of a closed membrane rubber box.

To further investigate the effect of the earth pressure and the rock socketing depth, the distribution of earth pressure, wall displacement, and bending moment during the time of first water feeding are shown in Figures 12 & 13. Figure 12 shows the variation of normalized effective earth pressure at the deepest depth with wall displacement at different water levels. The deepest earth pressure cell has been

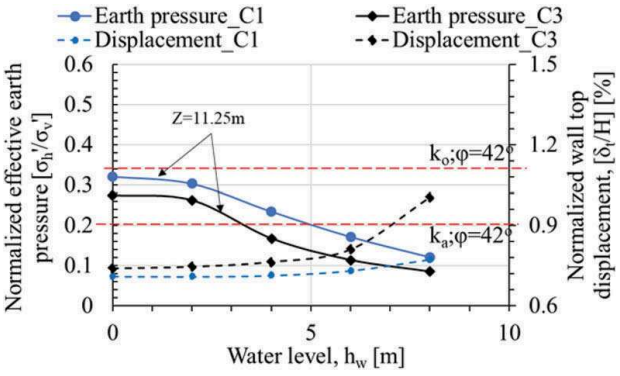

Figure 12. Earth pressure and wall displacement variation during static loading (water rise).

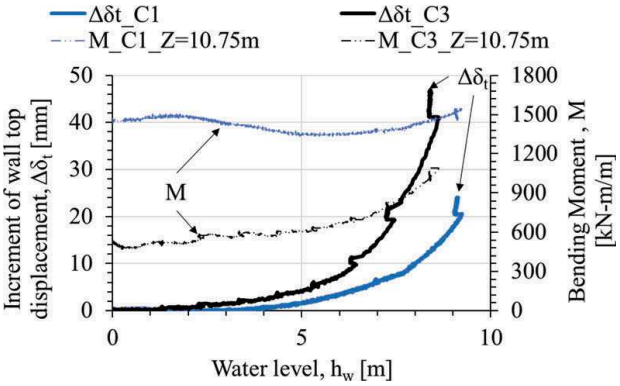

Figure 13. Increment of wall displacement and bending moment variation during static loading (water rise).

considered as the water start to fill from bottom to top. When h_w=0m the normalized effective earth pressure of case 1 is higher than case 3 which indicates the effect of the loading history on the accumulation of the earth pressure along with the effect of 0.5m rock socketing depth. As the water level increases, the effective earth pressure starts to decrease from at-rest to active condition though the wall displacement does not change significantly. The wall displacement starts to increase significantly after a certain water level which can be explained by the increase of bending moment after a certain water level (see Figure 13). At the end of the water feeding, the wall displacement experienced in case 1 is smaller than case 3 which indicates the effect of the 0.5m rock socketing depth.

To further study the effect of the rock socketing depth on the overall behavior of case 1 and case 3, the bending moment and earth pressure relationship to the wall top displacement are shown in Figures 14 & 15. Figure 14 shows the residual bending moment (M_r) relationship to the residual wall top displacement (δ_{tr}). For the comparison purpose the strain gauge which is located in the same distance from the rock surface (1.25m from rock surface) for case 1 and 3 have been considered. It is seen that the wall displacement increases as the bending moment

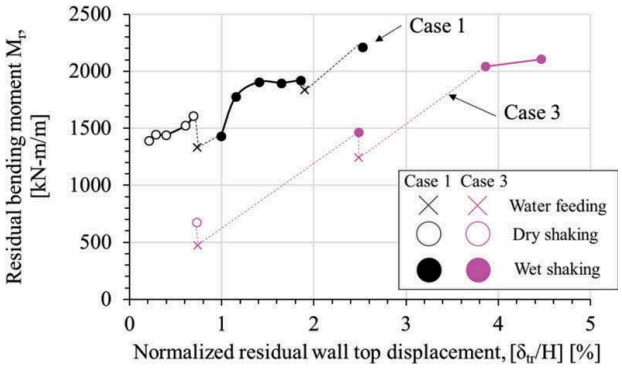

Figure 14. Relationship between residual wall displacement and residual bending moment (at 1.25m from rock surface).

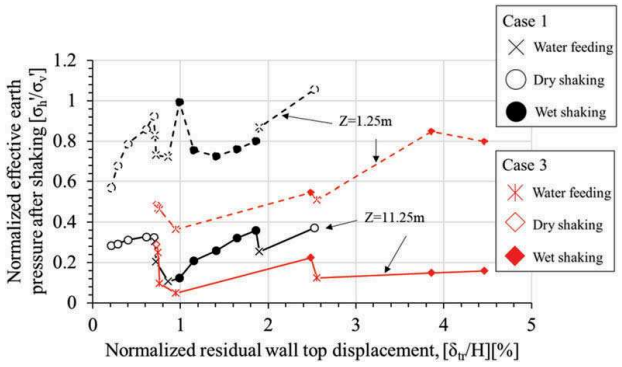

Figure 15. Relationship between residual wall displacement and residual earth pressure at shallow and deepest depth.

increases, which mean the force behind the wall has increased. The increase of the residual bending moment can be explained by the increase of the residual earth pressure shown in Figure 15. As seen in Figures 10 and 11, the earth pressure at the top half is more critical than the bottom half, because the earth pressure at the top part is higher than the reference K_o pressure, where the bottom half is close to K_o pressure. So, to further understand the earth pressure variation at shallow and deepest depth, the residual effective earth pressure at z=1.25 & 11.25 m is plotted against the residual wall top displacement in Figure 15. The earth pressure has been normalized by effective vertical earth pressure (σ_v') to understand the behavior more clearly. It is seen that the earth pressure at shallow depth increases significantly than the deepest depth. In case 1, the earth pressure at shallow and deepest depth increases from the first shaking till the last shaking which causes the gradual increase of the residual bending moment as observed in Figure 14. Similarly, in case 3, the earth pressure at shallow and deepest depth increase from the first shaking till the last shaking in the deepest depth but decreases between the shake 3 & 4 at the shallow depth which causes an overall small increase in the bending moment between shake 3 and 4. Though case 3 has large wall displacement but the bending moment of case 3 is much smaller than case 1, which means that the reaction given by 3m socketing wall is higher than a 2.5m wall. Also, the increase of the bending moment at the final shaking proves that the rock confinement can still provide resistance to the applied load. However, considering the bending moment of the final shaking of case 1 & 3, it is confirmed that the wall with a 3m socketing depth has more resilience left compared to case 3.

According to Wu and Prakash (1996), the failure by horizontal wall displacement will take place at 10%H. Huang et al. (2009) limit the seismic displacement criterion based on the soil strength mobilization and proposed that 5%H can be considered as a significant wall movement to cause failure. According to the IPA (2016) standard, on the top of the sheet pile wall should not exceed 1%H in normal condition and 1.5%H under Level 1 seismic motion. From Figure 14 & 15 it is seen that, case 1 can withstand many shakings before reaching to the allowable limit provided by IPA (2016) standard but in case 3 the wall almost reaches to the allowable limit (about 0.8%H) just after 1 shake confirming the significant effect of change in 0.5m rock socketing depth.

Figure 16 shows the observed crack and deformation of the soft rock after each test. Considering the post softening characteristics in the stress-strain behavior of the soft rock, catastrophic failure was expected during the experiment. Though the wall displacement experience by case 3 is almost close to 5%H yet no catastrophic failure was observed. One of the possible reasons could be the presence of large overburden pressure (about 180kPa for dry and

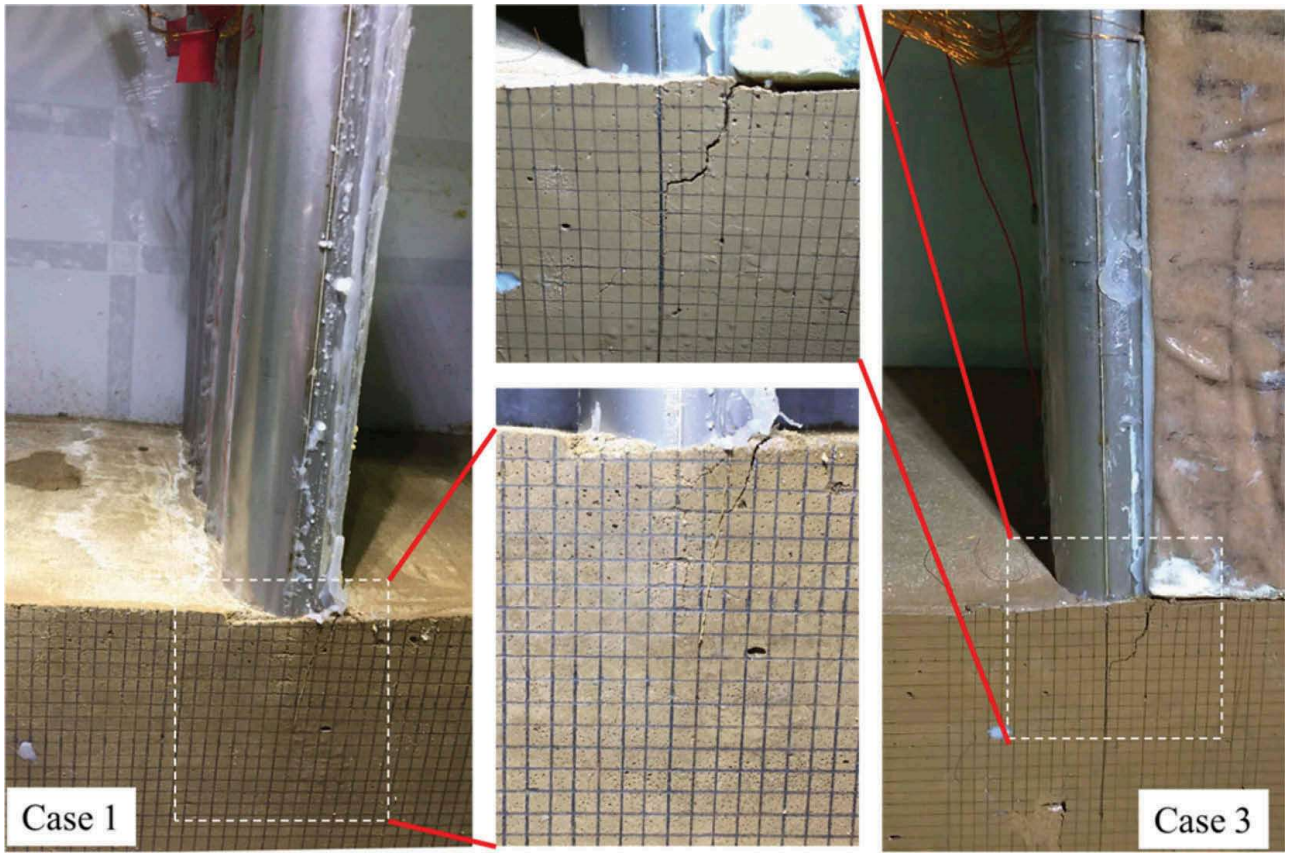

Figure 16. Observed crack and deformation of the soft rock after the test.

240 kPa for wet) due to the large retain height which prevents the wall from undergoing any catastrophic failure.

4 CONCLUSION

The main intention of this model study is to investigate the dynamic stability of a steel tubular pile wall embedded in soft rock with relatively small embedment depth than Chang's proposed minimum depth and observe the deformation and failure behaviors. The d_e=3m and 2.5m were considered for this study and the effect of 0.5m change in the embedment depth are discussed in this paper. Based on the discussion following conclusion can be drawn:

1. Under similar test conditions, when two similar earthquake loads are applied, the wall displacement will be smaller for the second loading than the first loading meaning the wall resilience will increase in the second loading.
2. The performances of the wall are considerably improved by the increase of the depth of the rock socketing by 0.5 m.
3. Although the wall with d_e=2.5m had a displacement of approximately 4.5%H, there were no catastrophic failures, demonstrating that d_e=2.5m can provide an adequate margin of safety to avoid catastrophic failures even under level 2 earthquake.
4. The earth pressure at the upper half of the wall is very critical relative to the lower half. However, the experience of earth pressure through the wall with d_e=3m is higher than the wall with d_e=2.5m which means that the resistance provided by the rock with d_e=3m is higher than d_e=2.5m.
5. The loading history has a significant effect on the earth pressure behavior that has been confirmed in dynamic and static events. During dynamic loading, residual earth pressure accumulates with an increase in wall displacement. The accumulation of the residual earth pressure of the wall with d_e=3m is greater than the wall with d_e=2.5m confirming the effect of 0.5m of change in the depth of the rock socketing.
6. Contrary to the dynamic load, the earth pressure tends to decrease with the increase in the displacement of the walls during the static load. The reduction of earth pressure takes place at a very small change in the displacement. However, the movement will begin to change considerably once the water level reaches a certain level.

ACKNOWLEDGEMENT

The authors gratefully acknowledge the individual advice and guidance provided by the members and advisers of the IPA TC1 (Committee on the application of cantilever type steel tubular pile wall

embedded to the stiff ground) in connection with the preparation of this paper.

REFERENCES

Bica, A. V. D. & Clayton, C. R. I. 1998. An experimental study of the behaviour of embedded lengths of cantilever walls. *Geotechnique* 48(6), 731–745.

Chang, Y.L. 1937. Lateral pile loading tests. *Transaction of American Society of Civil Engineering* 102, 273–276.

Huang, C.-C., Wu, S.-H. & Wu, H.J. 2009. Seismic Displacement Criterion for Soil Retaining Walls Based on Soil Strength Mobilization. *Journal of Geotechnical and Geoenvironmental Engineering* 135:74–83.

International Press-in Association (IPA), 2016. Press-in Retaining Structures: a handbook, 1st ed. AD II–76

Jo, S., Ha, J., Yoo, M., Choo, Y.W., & Kim, D. 2014. Seismic behavior of an inverted T-shape flexible retaining wall via dynamic centrifuge tests. *Bull Earthquake Engineering* 12:961–980. DOI 10.1007/s10518-013-9558-9.

Jo, S., Ha, J., Lee, J. & Kim, D. 2017. Evaluation of the seismic earth pressure for inverted T-shape stiff retaining wall in cohesionless soils via dynamic centrifuge. *Soil dynamics and earthquake engineering* 92, 345–357. http://dx.doi.org/10.1016/j.soildyn.2016.10.009.

Kunasegaram, V., Shafi, S.M., Takemura, J. & Ishihama, Y., 2019. Centrifuge model study on cantilever steel tubular pile wall embedded in soft rock. *Geotechnique for sustainable infrastructure development, Lecture Notes in Civil Engineering 62*, https://doi.org/10.1007/978-981-15-2184-3_135

Kunasegaram, V. & Takemura, J. 2019. Deflection and failure of high stiffness cantilever retaining wall embedded in soft rock. *International Journal of Physical Modelling in Geotechnics*, https://doi.org/10.1680/jphmg.19.00008

Madabhushi, S.P.G. & Chandrasekaran, V.S. 2005. Rotation of cantilever sheet pile walls. *Journal of Geotechnical and Geoenvironmental Engineering* 131(2), 202–212.

Madabhushi, S.P.G. & Zeng, X. 2006. Seismic response of flexible cantilever retaining walls with dry backfill. *Geomechanics and Geoengineering: An International Journal* 1(4), 275–289.

Mononobe, N. & Matsuo, M. 1929. On the determination of earth pressures during earthquakes. *Proceedings: World Engineering Conference*, Japan, Vol. 9.

Tatsuoka, F., Goto, S. & Sakamoto, M. 1986. Effects of some factors on strength and deformation characteristics of sand at low pressures. *Soils and Foundations* 26(1): 105–114.

Terzaghi, K. 1934a. Large retaining wall tests. I. Pressure of dry sand. *Engineering News-Rec*. 136–140.

Terzaghi, K. 1934b. Large retaining wall tests. II. Pressure of dry sand. *Engineering News-Rec*. 259–262.

Viswanadham, B., Madabhushi, S. Babu, K. & Chandrasekaran, V. 2009. Modelling the failure of a cantilever sheet pile wall. *International Journal of Geotechnical Engineering* 3:2, 215–231, DOI: 10.3328/IJGE.2009.03.02.215-231

Wu, Y. & Prakash, S. 1996. On seismic displacements of rigid retaining walls. *ASCE Geotechnical Special Publication: Analysis and Design of Retaining Structures Against Earthquakes*, S. Prakash, ed., ASCE, New York, 21–37.